J Bioenerg Biomembr (2010) 42:311–320
DOI 10.1007/s10863-010-9298-3

Crystal and solution structure of the C-terminal part of the *Methanocaldococcus jannaschii* A_1A_O ATP synthase subunit E revealed by X-ray diffraction and small-angle X-ray scattering

Asha Manikkoth Balakrishna · Malathy Sony Subramanian Manimekalai · Cornelia Hunke · Shovanlal Gayen · Manfred Rössle · Jeyaraman Jeyakanthan · Gerhard Grüber

Received: 23 March 2010 / Accepted: 23 May 2010 / Published online: 23 June 2010

Abstract The structure of the C-terminus of subunit E ($E_{101–206}$) of *Methanocaldococcus jannaschii* A-ATP synthase was determined at 4.1 Å. $E_{101–206}$ consist of a N-terminal globular domain with three α-helices and four antiparallel β-strands and an α-helix at the very C-terminus. Comparison of *M. jannaschii* $E_{101–206}$ with the C-terminus $E_{81–198}$ subunit E from *Pyrococcus horikoshii* OT3 revealed that the kink in the C-terminal α-helix of $E_{81–198}$, involved in dimer formation, is absent in *M. jannaschii* $E_{101–206}$. Whereas a major dimeric surface interface is present between the *P. horikoshii* $E_{81–198}$ molecules in the asymmetric unit, no such interaction could be found in the *M. jannaschii* $E_{101–206}$ molecules. To verify the oligomeric behaviour, the low resolution structure of the recombinant $E_{85–206}$ from *M. jannaschii* was determined using small angle X-ray scattering. Rigid body modeling of two copies of one of the monomer established a fit with a tail to tail arrangement.

Keywords Crystallization · Small angle X-ray scattering · Subunit E · A_1A_O ATP synthase · Archaea

Electronic supplementary material The online version of this article (doi:10.1007/s10863-010-9298-3) contains supplementary material, which is available to authorized users.

A. M. Balakrishna · M. S. S. Manimekalai · C. Hunke · S. Gayen · G. Grüber (✉)
School of Biological Sciences,
Nanyang Technological University,
Singapore 637551, Republic of Singapore
e-mail: ggrueber@ntu.edu.sg

M. Rössle
European Molecular Biology Laboratory, Hamburg Outstation,
EMBL c/o DESY,
22603 Hamburg, Germany

J. Jeyakanthan
National Synchrotron Radiation Research Center,
101 Hsin-Ann Road, Hsinchu Science Park,
Hsinchu 30076, Taiwan

Introduction

Archaea synthesize adenosine triphosphate (ATP) from adenosine diphosphate (ADP) and inorganic phosphate by a so-called A_1A_O ATP synthase that is distinct from the known F_1F_O ATP synthases occurring in eubacteria, mitochondria, and chloroplasts. The overall structure of A_1A_O ATP synthase can be divided into a cytoplasmic A_1 domain that catalyzes ATP synthesis and an integral membrane part, A_O, that serves as an ion channel (Lewalter and Müller 2006; Grüber and Marshansky 2008). The A_1 sector is elongated, with an A_3:B_3 headpiece, in which catalysis takes place, and an elongated stalk (Grüber et al. 2002), composed by the subunits C, D, and F (Coskun et al. 2002; Coskun et al. 2004a). Two and three dimensional reconstructions of the A_1A_O ATP synthase, obtained by single particle analysis, revealed two peripheral stalks, and a collar-like structure (Chaban et al. 2002; Coskun et al. 2004a; Bernal and Stock 2004; Vonck et al. 2009), proposed to be composed of the subunits H, E and *a*, (Coskun et al. 2004a; Schäfer et al. 2006a). Both the peripheral stalks and the collar-like structure are believed to be involved in constituting the stator region of the enzyme, which is predicted to have important roles in enzyme assembly as well as energy coupling between A_1 and A_O sectors (Schäfer

et al. 2006b; Grüber and Marshansky 2008). The low resolution structure of subunit H of the A_1A_O ATP synthase from *Methanocaldococcus jannaschii* has been determined from small angle X-ray scattering data (Biuković et al. 2007). Subunit H is dimeric in solution (Biuković et al. 2007, 2009) and has a boomerang-like shape, which is divided into two arms of 120 Å and 60 Å in length (Biuković et al. 2007). An NMR solution structure of the 60 Å long N-terminal arm (Biuković et al. 2009) and the C-terminal segment $H_{85–104}$ of subunit H from *M. jannaschii* A_1A_O ATP synthase have been solved (Gayen and Grüber 2010), revealing α-helical features. Subunit H is described to be partially associated with subunit E, an assembly formation, which is an important factor in the stabilization and formation of the stator in A-ATP synthases (Müller and Grüber 2003; Gayen et al. 2008; Kish-Trier and Wilkens 2009; Gayen and Grüber 2010). NMR titration experiments described that $H_{1–47}$ interacts with the N-terminal segment of subunit E (Gayen et al. 2008) via a proposed helix–helix formation (Gayen et al. 2008; Biuković et al. 2009), which has been confirmed by the NMR solution structure of the N-terminal segment $E_{1–52}$ of the *M. jannaschii* subunit E (Fig. 1; Gayen et al. 2009). Previously, the 198 amino acid subunit E from *Pyrococcus horikoshii* OT3 has been crystallized, whereby the entire N-terminal domain of 80 amino acids was autocatalytically cleaved during crystallization, and only the truncated C-terminal part (residues 81–198), $E_{81–198}$, crystallized (Lokanath et al. 2007). The determined structure showed $E_{81–198}$ composed of four antiparallel β-strands and six α-helices (Fig. 1; Lokanath et al. 2007). In this structure *P. horikoshii* OT3 $E_{81–198}$ forms two types of dimers, a strong homodimer via a major interface and a weak dimer with a minor interface. Because of low reproducibility and low level expression, attempts to examine the oligomeric state of the C-terminal domain in solution and its relative orientation to the N-terminal tail of subunit E were hampered (Lokanath et al. 2007).

Here we made use of our recently and presently generated C-terminal recombinant proteins $E_{101–206}$ (Gayen et al. 2008) and $E_{85–206}$ of the A-ATP synthase from *M.*

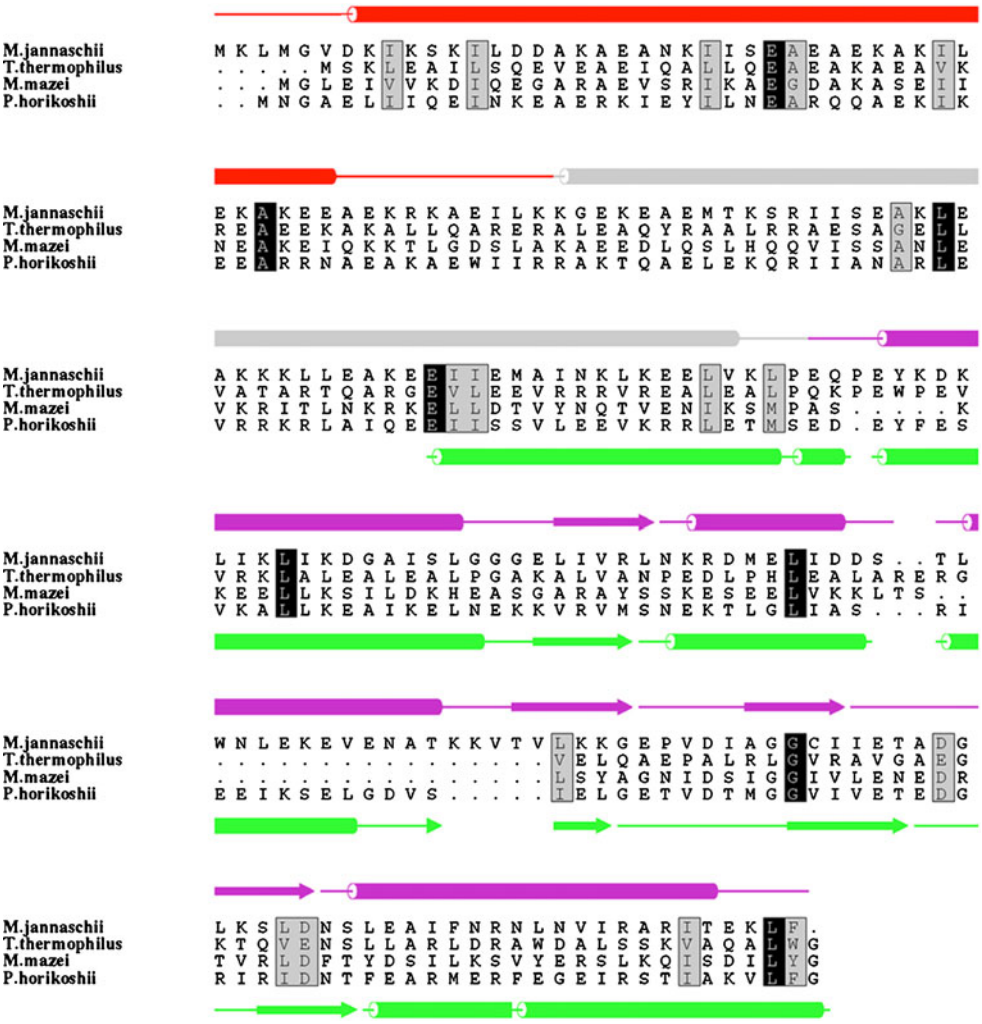

Fig. 1 Multiple sequence alignment of subunit E of A_1A_O ATP synthases from *M. jannaschii*, *Thermus thermophilus*, *Methanosarcina mazei* Gö1 and *P. horikoshii* OT3. The secondary structure of the N-terminal α-helical structure of *M. jannaschii* $E_{1–52}$ (*red*, PDB code 2KK7, (Gayen et al. 2009)) was derived from NMR experiments. The secondary structures based on the crystallographic models of *P. horikoshii* OT3 $E_{81–198}$, (*green*, PDB code 2DM9 (Lokanath et al. 2007)) and *M. jannaschii* $E_{101–206}$ (*magenta*) presented here, were aligned to a selection of homologous structures. The predicted assignment for $E_{53–100}$ is shown in *grey colour*

jannaschii and determined the crystallographic and low resolution structures, respectively, to address the question of structural similarities and diversities of the C-terminal domains resolved so far, and to get insight into the oligomeric state of subunit E in solution. Due to the availability of the two structures $E_{1–52}$ (Gayen et al. 2009) and $E_{101–206}$ from the same species, *M. jannaschii* subunit E, NMR titration experiments have been performed to address the possible arrangement of both tail segments inside subunit E.

Experimental procedures

Cloning and overexpression

In order to amplify the truncated construct of *M. jannaschii* subunit E, $E_{85–206}$, the primers 5′ - GTT GCC ATG GCT GTG AAA TTG ATG GGA - 3′ (forward primer) and 5′ - CTC CGA GCTC TCA TGG CAG TTT AAC - 3′ (reverse primer) were designed. The underlined bases represent the restriction enzyme cleavage sites. The genomic DNA from *M. jannaschii* ATCC® #43067D™ was used as the template. Following digestion with *Nco*I and *Sac*I, the PCR products were ligated into the pET9d1-His_3 vector (Grüber et al. 2002). The insert-containing pET9d-His_3 vector was transformed into *Escherichia coli* cells (strain BL21(DE3)). To express the respective proteins, liquid cultures were grown at 37 °C in LB medium containing kanamycin (30 μg/ml) until an optical density OD_{600} of 0.6–0.7 was reached. Cultures were supplemented with isopropyl-β-D-thiogalactopyranoside to a final concentration of 1 mM, to induce production of proteins, followed by incubation for another 4 h at 37 °C.

Protein purification

Bacterial cells containing the recombinant $E_{85–206}$ from *M. jannaschii* were harvested from 2 l cultures by centrifugation at 8,000 × g for 10 min at 6 °C. The cells were lysed on ice in buffer A (50 mM Tris, pH 7.5, 150 mM NaCl, 1 mM PMSF, 4 mM Pefabloc^{SC}) by sonication with an Ultrasonic Homogenizer (Bandelin, Tip KE76) for 3× 1 min. After sonication the cell lysate was heated for 20 min at 70 °C, followed by centrifugation at 10,000 × g for 35 min at 4 °C. The resulting supernatant was passed through a filter (0.45 mm pore-size) and supplemented with Ni^{2+}-NTA resin. The His-tagged protein was allowed to bind to the matrix for 2 h at 4 °C by mixing on a sample rotator (Neolab), and eluted with an imidazole-gradient (0–250 mM) in buffer A. Fractions containing required protein were identified by SDS-PAGE (Laemmli 1970), pooled and concentrated using a Millipore spin concentrator with a molecular mass cut-off of 3 kDa. The sample was applied on a gel filtration column Superdex HR75 (10/30, GE Healthcare). Respective fractions were concentrated in Millipore spin concentrators. The purity of the protein sample was analyzed by SDS-PAGE (Laemmli 1970). The SDS-PAGE was stained with Coomassie Brilliant Blue R250. The recombinant proteins $E_{1–52}$ and $E_{101–206}$ from *M. jannaschii* have been isolated according to Gayen et al. (2008, 2009).

Circular dichroism spectroscopy

Steady state CD spectra were measured in the far UV-light (185–260 nm) using a CHIRASCAN spectropolarimeter (Applied Photophysics) according to Biuković et al. (2007).

Crystallization conditions

The purified $E_{101–206}$ from *M. jannaschii* was concentrated to 8–10 mg/ml in buffer B (50 mM Hepes, pH 7.0 and 75 mM NaCl) using a 3 kDa cutoff concentrator. Preliminary screening for initial crystallization conditions were performed using Hampton crystal screen 1 and 2 using the vapour diffusion technique. Hanging drops were set by mixing 1 μl of the concentrated protein solution in buffer B with an equal volume of reservoir solution in a 24-well VDX plates (Hampton Research, USA) and incubated at 291 K. Crystals of good diffraction quality appeared in about 5 days from a condition with 0.05 M Cesium chloride, 0.1 M MES monohydrate buffer, pH 6.5, 30% (*v*/*v*) Jeffamine M-600 and 1 mM Tris(2-carboxyethyl)phosphine (TCEP) of the Crystal screen 2 and these were further optimized by systematically adjusting the protein concentrations and additives. Finally, the optimized native crystals were grown in 10 mg/ml protein concentration in 0.05 M Cesium chloride, 0.1 M MES monohydrate buffer, pH 6.5, 30% (*v*/*v*) Jeffamine M-600, 1 mM TCEP and 0.1 ul of 0.05 M glycine as additive. The crystals were flash-frozen in liquid nitrogen at 100 K.

X-ray diffraction and data analysis of the protein crystal $E_{101–206}$

Datasets for $E_{101–206}$ crystals were collected at 100 K in SPring-8 RIKEN Beamline 26B2 (SPring-8, Japan) using Mar CCD 225 detector. All the diffraction data were indexed, integrated and scaled using the HKL2000 suite of programs (Otwinowski and Minor 1997). The details of the data collection statistics are given in Table 1. All crystals belong to hexagonal space group $P6_122$.

The structure of the C-terminal segment of subunit E, $E_{81–198}$, of *P. horikoshii* OT3 (PDB code 2DM9 (Lokanath et al. 2007)) was used as a model for the structure

Table 1 Statistics of crystallographic data collection and refinement for subunit $E_{101–206}$

Data collection statistics	
Wavelength (Å)	1.0
Space group	$P6_122$
Unit cell parameters (Å)	
a = b =	73.66
c =	149.64
α = β (°) =	90
γ (°) =	120
Resolution range (Å)	30.0–4.1
Solvent content (%)	51.21
Number of unique reflections	4,717
I/σ[a]	27.35 (26.35)
Completeness (%)	99.3 (100.0)
R merge[b] (%)	6.8 (7.6)
Multiplicity	10.8 (11.5)
Refinement statistics	
R factor[c] (%)	35.27
R free[d] (%)	38.12
Number of amino acid residues	212
Ramachandran statistics	
Most favored (%)	71.3
Additionally allowed (%)	23.9
Generously (%)	4.8
Disallowed (%)	0.0
R.M.S. deviations	
Bond lengths (Å)	0.004
Bond angles (º)	0.847
Mean atomic B values	
Overall	26.5
Wilson	73.4

[a] Values in parentheses refer to the corresponding values of the highest resolution shell (4.17–4.1 Å)

[b] $R_{merge} = \sum\sum_i |I_h - I_{hi}| / \sum\sum_i I_h$, where I_h is the mean intensity for reflection h

[c] $R - factor = \sum ||F_O| - |F_C|| / \sum |F_O|$, where F_O and F_C are measured and calculated structure factors, respectively

[d] $R - free = \sum ||F_O| - |F_C|| / \sum |F_O|$, calculated from 5% of the reflections selected randomly and omitted from the refinement process

determination by molecular replacement method using the program PHASER (McCoy et al. 2007). Two molecules were located in the asymmetric unit. Rigid body refinement was carried out followed by restrained refinement with tight geometric restraints. Iterative cycles of model building and refinement were carried out using the programs COOT (Emsley and Cowtan 2004) and REFMAC5 (Murshudov et al. 1997) of the CCP4 suite (1994) until convergence. The geometry of the final models was checked with PROCHECK (Laskowski et al. 1993) and the figures are drawn using the program PyMOL (DeLano 2002). Structural comparison analysis are carried out using the SUPERPOSE program (Krissinel and Henrick 2004) and the solvent accessible areas were calculated using the AREAIMOL program (Saff and Kuijlaars 1997) as included in the CCP4 suite. The atomic coordinates and structure factors have been deposited in the Protein Data Bank under accession code 3LG8.

Small angle X-ray scattering experiments and data analysis

The synchrotron radiation X-ray scattering data of $E_{85–206}$ from *M. jannaschii* were collected at the updated X33 beamline (Boulin et al. 1986; Roessle et al. 2007) using a MAR345 image plate detector (MarResearch, Norderstedt, Germany) of the EMBL-Outstation Hamburg located on a bending magnet (sector D) on the storage ring DORIS III of the Deutsches Elektronen Synchrotron (DESY). A photon counting Pilatus 1 M pixel detector (67×420 mm^2) was used at a sample—detector distance of 2.4 m covering the range of momentum transfer $0.1 < s < 4.5$ nm^{-1} ($s=4p \sin(q)/l$, where q is the scattering angle and l=0.15 nm is the X-ray wavelength). The S-axis was calibrated by the scattering pattern of Silver-behenate salt (d-spacing 5.84 nm). The scattering patterns from subunit α were measured at protein concentrations of 2.0 and 8.0 mg/ml, respectively. Protein samples were prepared in 50 mM Tris/HCl (pH 7.5), 150 mM NaCl and 1.25 mM DTT as radical quencher and injected automatically using the sample-changing robot for solution scattering experiments at the SAXS station X33 (Round et al. 2008). The data were normalized to the intensity of the incident beam; the scattering of the buffer was subtracted and the difference curves were scaled for concentration. All the data processing steps were performed using the program package PRIMUS (Svergun 1993). The forward scattering *I(0)* and the radius of gyration R_g were evaluated using the Guinier approximation (Guinier and Fournet 1955).

The molecular mass of $E_{85–206}$ was calculated by comparison with the forward scattering from the reference solution of bovine serum albumin (BSA). From this procedure a relative calibration factor for the molecular mass (MM) can be calculated using the known molecular mass of BSA (66.4 kDa) and the concentration of the reference solution by applying

$$MM_p = I(0)_p / c_p \times \frac{MM_{st}}{I(0)_{st} / c_{st}}$$

where $I(0)_p$, $I(0)_{st}$ are the scattering intensities at zero angle of the studied and the BSA standard protein, respectively, MM_p, MM_{st} are the corresponding molecular masses and c_p, c_{st} are the concentrations. Errors have been calculated from the upper and the lower I(0) error limit estimated by the

Guinier approximation. The shape of $E_{85–206}$ in solution was built by the program DAMMIN as described by Svergun (1999).

NMR-titration experiments

In order to analyze a possible interaction between the N- and C-terminal part of subunit E, a series of ^{1}H - ^{15}N heteronuclear single quantum coherence (HSQC) spectra were recorded at 298 K for the fixed concentration of 100 μM of $E_{101–206}$, titrated with increasing amounts (up to 1.5 equivalents) of $E_{1–52}$. The proteins were incubated for 30 mins for binding during each step of the experiment. The change in chemical shift was monitored in the HSQC spectra. All the samples used were buffer exchanged finally with a 25 mM sodium phosphate (pH 6.5) buffer prior to the binding experiments.

Results and discussion

Crystallization and X-ray analysis of $E_{101–206}$ from *M. jannaschii*

Crystals of the C-terminal part of subunit E, $E_{101–206}$, from *M. jannaschii* (Supplementary Fig. S1A) diffracted to 4.1 Å resolution (Supplementary Fig. S1B) and belong to the space group $P6_122$, with unit-cell parameters $a=b=$ 74.24 Å, $c=149.62$ Å. Assuming two molecules in the asymmetric unit, the solvent content is 51.21% and V_m is 2.52 $Å^3$ per Dalton (Matthews 1968). The phase was obtained using the crystal structure of the C-terminal domain, $E_{81–198}$, of subunit E from *P. horikoshii* OT3 (PDB code 2DM9) (Lokanath et al. 2007), whereby the globular head domain containing residues 101–169 was used for initial phasing.

Crystallographic structure of $E_{101–206}$

The crystal structure of $E_{101–206}$ from *M. jannaschii* was determined to a resolution of 4.1 Å (Fig. 2a). Two molecules were identified in the asymmetric unit and the initial phases were improved by many cycles of density modification using the program DM from CCP4 (Cowtan 1994). The resultant electron density map clearly showed the elongated part of the C-terminal helix, which was manually built using COOT (Emsley and Cowtan 2004).

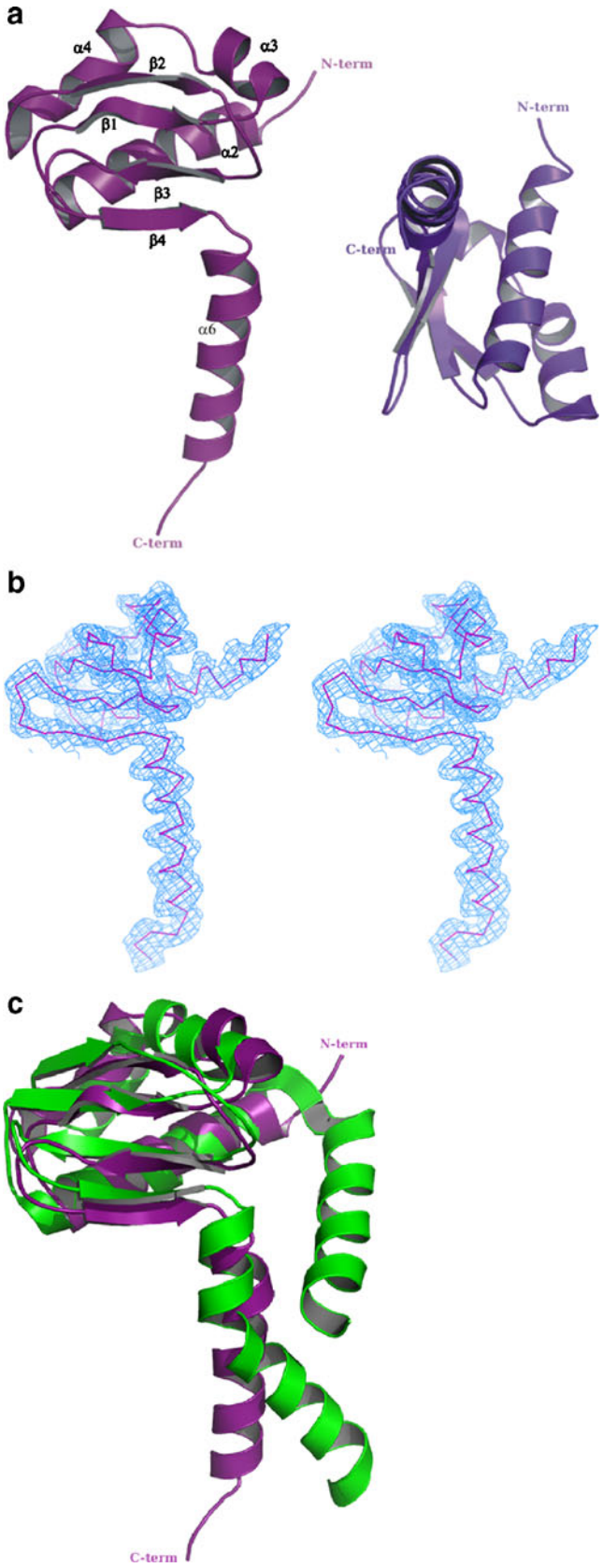

Fig. 2 **a** Crystallographic structure of *M. jannaschii* $E_{101–206}$, chain A is shown as magenta and chain B in purple. **b** Stereoview of the electron density map (2Fo-Fc) of chain A at 1σ for $E_{101–206}$. **c** Superposition of the *M. jannaschii* $E_{101–206}$ with the C-terminal domain of subunit E, $E_{81–198}$, of *P. horikoshii* OT3 shown in green colour (PDB code 2DM9 (Lokanath et al. 2007))

Many cycles of model building and restrained refinement with tight geometric restraints were carried using overall temperature factor and Non-Crystallographic Symmetry (NCS) restraints. The details of the refinement statistics are presented in Table 1. The final electron density map for the main chain atoms are excellent (Fig. 2b), whereas for the side chain atoms no visible densities could be identified.

The overall structure of $E_{101–206}$ has dimensions of 53 Å×32 Å×20 Å and consists of two segments, the N-terminal α-β globular head part, including amino acids 101–184 with three α-helices and four antiparallel β-strands and the C-terminal elongated tail with a single α-helix, formed by the amino acids residues 185–206 (Fig. 2a). The structure is similar to the C-terminal segment, $E_{81–198}$, of subunit E from *P. horikoshii* OT3 (Lokanath et al. 2007) and they superimpose with an r.m.s deviation of 5.76 Å for the backbone Cα atoms of the globular head domain (101–184) (Fig. 2c), reflecting the amino acid identity and homology of 31% and 54%, respectively (Fig. 1) for the entire E subunits from both organisms. Larger than average deviations are observed for regions Ile118-Leu125 (the loop region after the N-terminal helix) and Val149-Lys180 (containing the four antiparallel β-strands). The very C-terminal helix of $E_{101–206}$ and $E_{81–198}$ is the most deviating part, moving away by around 7 Å (Fig. 2c). In addition, a bend determined at amino acid Arg183 of the C-terminal α-helix of *P. horikoshii* $E_{81–198}$ was not observed in the $E_{101–206}$ structure, where it stays as a straight elongated helix. Analysis of the amino acids near the kink region in the *P. horikoshii* $E_{81–198}$ structure did not show any special residues that might induce helical bending. Furthermore as demonstrated in the recently published EG dimer structure of *Thermus thermophilus* A_1A_O ATP synthase (Lee et al. 2010) it might be concluded that the differences in the C-terminal helices of both the E-subunit structures could be caused by differences in their crystal lattice arrangement.

Comparison of the molecular arrangement of $E_{101–206}$ and $E_{81–198}$ in the asymmetric unit

The two monomers in the asymmetric unit of the *M. jannaschii* $E_{101–206}$ have an r.m.s. deviation of 0.598 Å and are rotated by approximately 70° with almost no interaction between them (Fig. 2a). As presented in Fig. 3, two dimer interfaces could be determined between the symmetry related molecules of $E_{101–206}$, one made-up by the tail helices, called the major dimer, and the other through the β-sheets in the globular head part, called minor dimer. Similar dimeric arrangements are also noted in *P. horikoshii* $E_{81–198}$ structure wherein the major dimer is formed within the two molecules in the asymmetric unit with the very C-terminal and the N-terminal helices of each molecule interacting in

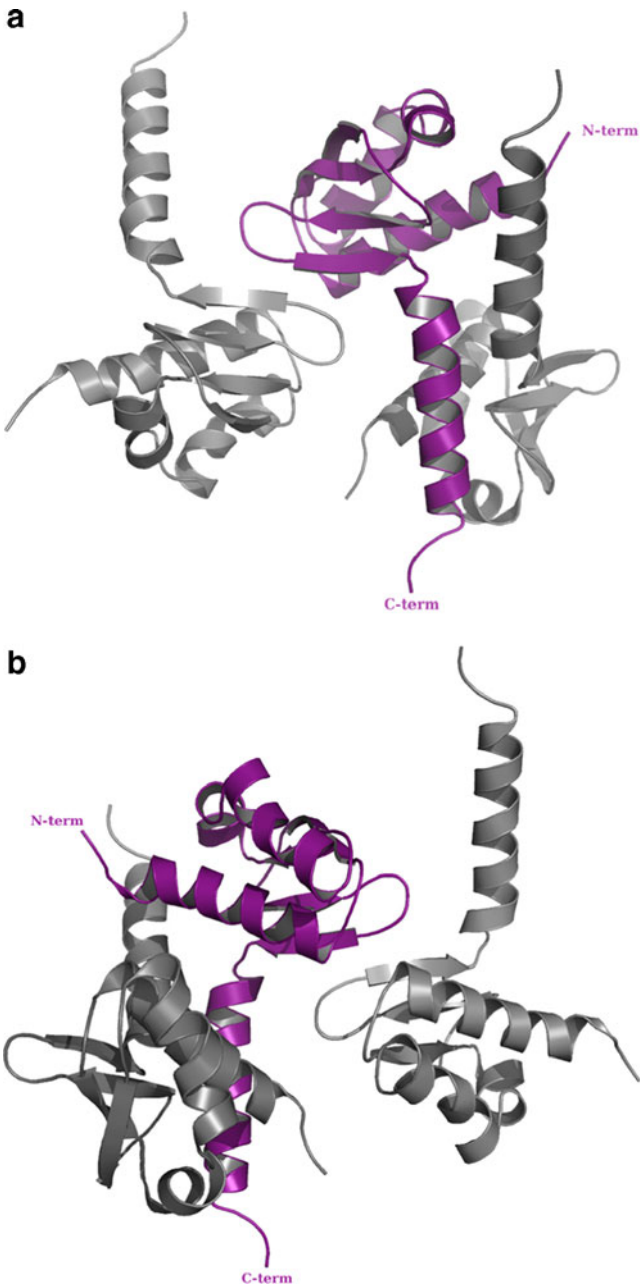

Fig. 3 The dimers formed by symmetry related molecules (*gray*) are shown for chain A (*magenta*) of $E_{101–206}$ from *M. jannaschii*. The major dimer interacts through the C-terminal helix and the minor dimer interacts via the N-terminal globular domain **a** view rotated by 180° **b**

the dimeric interface (Lokanath et al. 2007). A weak dimer is also formed with a symmetry related molecule by the β strand, $β_1$, giving a minor interface. The major dimeric interface has a significantly larger buried surface of 1,319 $Å^2$ while the minor dimeric interface has 464 $Å^2$ in the $E_{81–198}$ segment (Lokanath et al. 2007). However, unlike the *P. horikoshii* $E_{81–198}$ dimers, that has a vast difference in the buried surface area (855 $Å^2$), in the symmetry related dimer molecules of *M. jannaschii* $E_{101–206}$ the determined

buried surfaces are not only small with values of 221.7 Å^2 and 220.9 Å^2, respectively, but also very similar in size. Even though the buried surface area was calculated only for the back bone heavy atoms for *M. jannaschii* $E_{101–206}$ this might implicate that the smaller and weak dimers in *M. jannaschii* $E_{101–206}$ is due to crystal packing and that could also mean that the dimer formation in *P. horikoshii* $E_{81–198}$ could be because of crystal contact(s). This is so because it has already been shown for the subunit B of the *M. mazei* Gö1 ATP synthase that the crystallographic dimer formation for both B molecules in the asymmetric unit is not a true dimer although it has a large dimeric surface area of 2,304 Å^2 (Schäfer et al. 2006a). Inside the A_1A_O ATP synthase the B subunits are arranged in an alternating manner with the catalytic subunit A forming the A_3B_3 headpiece (Coskun et al. 2004b; Kumar et al. 2009).

Shape determination of *M. jannaschii* $E_{85–206}$ in solution

In order to understand in depth the oligomeric state of subunit E in solution, the recombinant protein $E_{85–206}$ from *M. jannaschii* has been generated, which is similar in size to the *P. horikoshii* $E_{81–198}$ protein. The recombinant $E_{85–206}$ was purified to high purity using affinity and size exclusion chromatography (Fig. S2A). The secondary structure of this subunit was determined from circular dichroism spectra (Fig. S2B). The overall spectrum is characteristic for a protein with mixed α/β-structure. The average secondary structure content is 56% α-helix, 21% β-sheet and 23% random coil, respectively, consistent with the secondary structure prediction, based on the amino acid sequence of *M. jannaschii* $E_{85–206}$ (Fig. 1).

The high purity of *M. jannaschii* $E_{85–206}$ allowed small-angle X-ray scattering (SAXS) experiments to be performed, with the aim to determine the first low resolution structure and the oligomeric state of this C-terminal domain in solution. SAXS patterns from solutions of the protein were recorded as described in Experimental procedures to yield the final composite scattering curve in Fig. 4a. Inspection of the Guinier plots at low angles indicated good data quality and no protein aggregation. The radius of gyration R_g of $E_{85–206}$ is 27.1±2 Å and the maximum dimension D_{max} of the protein is 94.6±2 Å (Fig. 4b). Comparison of the forward scattering with the values obtained for a reference in solution of BSA (66.4±2 kDa) yields a molecular mass of 23.6±2 kDa, which is about twice the value calculated from the amino acid sequence. The gross structure of $E_{85–206}$ was restored *ab initio* from the scattering pattern in Fig. 4a using the *ab initio* shape determination by simulated annealing modeling program DAMMIN, which fitted well to the experimental data in the entire scattering range (a typical fit displayed in Fig. 4a, curve 2, has the discrepancy χ=1.084). Ten independent reconstructions yielded reproducible models and the average and the most probable model is displayed in Fig. 4c. $E_{85–206}$ appears as an elongated molecule, composed of two similar domains of about 45.2 Å in length.

The molecular mass of 23.6±2 kDa clearly showed that the $E_{85–206}$ exists as dimer in solution. In order to compare the arrangement of the *M. jannaschii* $E_{101–206}$ molecules as found in the asymmetric unit and with respect to the neighbouring symmetry related molecules, both combinations were superimposed independently on the low resolution solution structure of $E_{85–206}$ from *M. jannaschii* (Supplementary Fig. S3A-B). It could be noted that none of the crystallographic arrangements do fit well into the solution structure, leaving out large masses unoccupied. The D_{max} values for the major and minor dimers are 56.3 Å and 66.8 Å, respectively. Many random orientations were tried for both molecular arrangements to fit into the solution structure but no best fit could be established. Finally, to assign the possible location of the two $E_{101–206}$ molecules in the solution shape, global rigid body modeling (Petoukhov and Svergun 2005) of two monomer structures of $E_{101–206}$ against the obtained scattering data revealed the two monomers arranged in a tail to tail orientation with very little interaction via the very C-terminal helix (Fig. 4d), the D_{max} of the model dimer being 82.2 Å. We also tried superimposing the *P. horikoshii* $E_{81–198}$ dimer structure (D_{max} being 75 Å) to the SAXS structure which yielded no good fitting (Supplementary Fig. S3C). Therefore, it could be concluded that the proximity of the *M. jannaschii* $E_{101–206}$ molecules in the asymmetric unit presented, may be caused by the crystallographic conditions. Furthermore, since the surface interface of the two molecules identified in solution envelope is small, it could be proposed that the entire subunit E from *M. jannaschii* might exist as a monomer in the enzyme, reflecting the ratio of 1:1 of subunit E with the single, rotary subunit D in the entire *M. jannaschii* A_1A_O ATP synthase complex (Coskun et al. 2004a).

Salt dependent molecular mass of *M. jannaschii* $E_{101–206}$ in solution

In order to prove, whether the surface interface of the two $E_{101–206}$ molecules is small, as calculated by the rigid body modeling, the salt content in the protein buffer has been increased to 500 mM NaCl. Subsequently the sample has been applied on a size exclusion column (Superdex HR75 (10/30, GE Healthcare)) to determine the molecular mass and the stoichiometry of *M. jannaschii* $E_{101–206}$. Comparison of the elution volume and the resulting *Kav* for $E_{101–206}$ form versus the standard protein lysozyme, with an apparent molecular mass of 14 kDa, suggests a native molecular mass of approximately 12±2 kDa (Fig. 5).

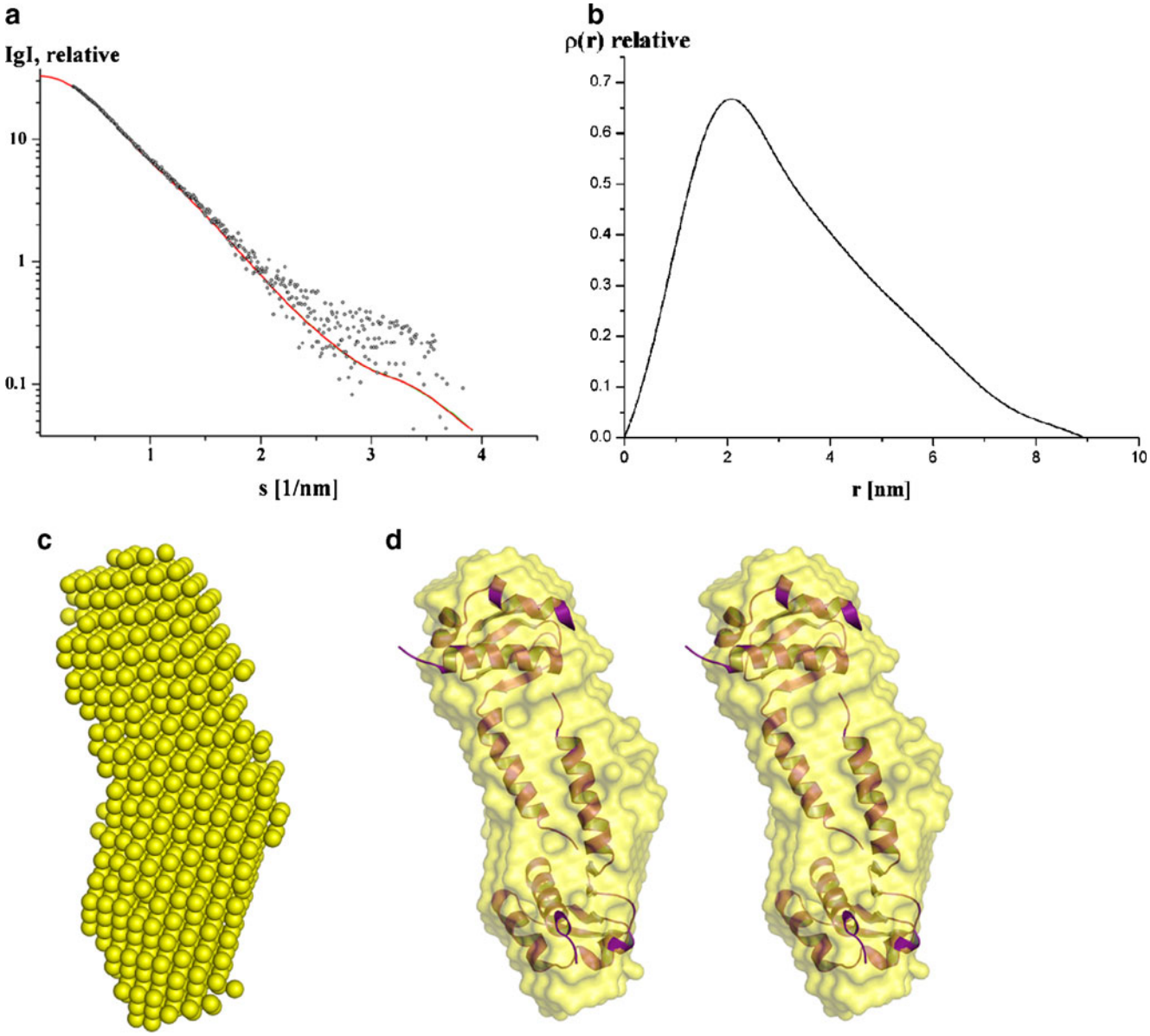

Fig. 4 Small Small-angle X-ray scattering data of $E_{85–206}$ from *M. jannaschii*. **a** Experimental scattering data (o) and the fitting curves (—; *green*: experimental, *red*: calculated from *ab initio* model) for $E_{85–206}$ from *M. jannaschii*. **b** The distance distribution function of the same protein. **c** Low resolution structure of $E_{85–206}$ in solution determined from SAXS data. **d** stereo view of the superposition of the DAMMIN model of $E_{85–206}$ from *M. jannaschii* (*yellow*) with the crystallographic structure of $E_{101–206}$ from *M. jannaschii*, based on the location and orientation of two $E_{101–206}$ monomers through rigid body modeling

Arrangement of the N-terminal helix $E_{1–52}$ and $E_{85–206}$ of *M. jannaschii*

NMR titration and fluorescence correlation experiments revealed that subunit E of the A_1A_O ATP synthase from *M. jannaschii* assembles via its N-terminal tail $E_{41–60}$ with residues in the N-terminus of subunit H (Gayen et al. 2008). The recently resolved NMR structure of the N-terminus $E_{1–52}$ of subunit E from *M. jannaschii* shows a hydrophobic strip in the α helical segment between residues 8–48, forming a surface for a possible hydrophobic and helix–helix interaction between subunit E and H and with the periodicity of Ala and/or Ile residues, indicating a coiled–coil interaction of both proteins (Gayen et al. 2009). However, in the absence of an entire structure of subunit E the arrangement of the *M. jannaschii* $E_{101–206}$ part relative to the remaining N-terminal tail, which is predicted to form a straight α-helix (Kish-Trier and Wilkens 2009), is unresolved so far. We examined the possibility of proximity of the globular part $E_{101–206}$ and the N-terminus of subunit E using NMR titration experiments. A 2D ^{1}H-^{15}N heteronuclear single quantum

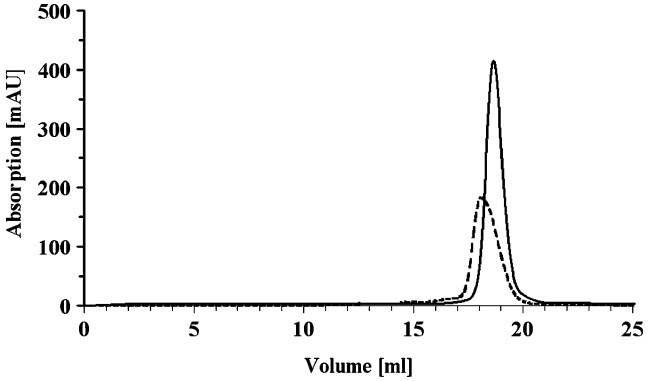

Fig. 5 Determination of native molecular mass by gel filtration analysis. Superdex 75 gel filtration analysis of $E_{101–206}$ from *M. jannaschii* (—) was applied and eluted (0.5 ml/min) using a buffer of 50 mM Hepes (pH 7.0), 500 mM NaCl, 10 mM EDTA and 1 mM DTT. Lysozyme ((– –), 14 kDa) has been used as molecular size standard

correlation (HSQC) spectrum of $E_{101–206}$ is revealed in Fig. 6a. When *M. jannaschii* $E_{1–52}$ was titrated to the labeled $E_{101–206}$ no significant chemical shift changes could be observed, indicating that there is no interaction between both proteins. Based on this result and the prediction of the N-terminal tail being a straight helix (Kish-Trier and Wilkens 2009), we have modeled the crystallographic structure of $E_{101–206}$ and the NMR-structure of $E_{1–52}$, resulting in a crosier-like shape of length 134 Å (Fig. 6b). The A_1 sector of the methanogenic A_1A_O ATP synthase is about 180 Å long, formed by the 94 Å high A_3B_3 headpiece and the 84 Å long central stalk, which covers the subunits C, D and F (Grüber et al. 2001; Coskun et al. 2004a). In this canon, subunit E, which has been shown to become crosslinked via its amino acid sequence 119 to 130 with the peptide 127 to 134 of the central subunit D in the entire A_1A_O ATP synthase using the zero-length crosslinker 1-ethyl-3-(dimethylamino-propyl)-carbodiimide (EDC (Schäfer et al. 2006b)), may not be able to span the entire length of 180 Å, as shown for the peripheral stalk subunit H from the same enzyme with a maximum dimension of 180 Å in solution (Biuković et al. 2007).

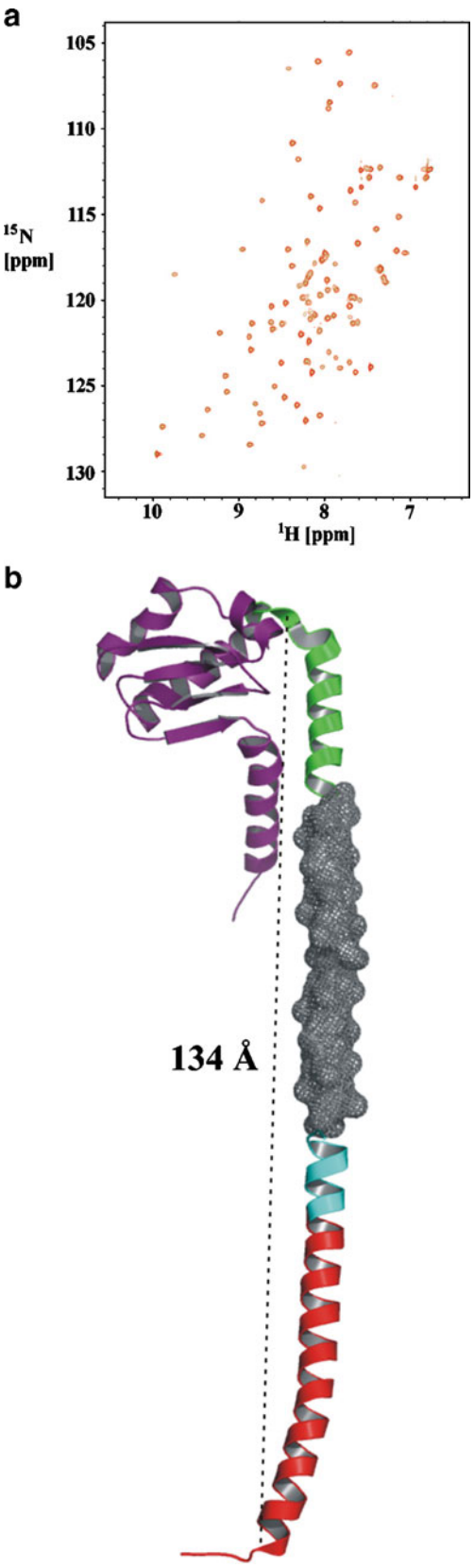

Fig. 6 **a** Overlay of 2D ^{1}H-^{15}N-HSQC spectra of $E_{101–206}$ from *M. jannaschii* in the absence (*red*) and presence (*green*) of 1.5 equivalent of unlabeled $E_{1–52}$. All the spectra were collected in a Bruker Avance 600 MHz spectrometer in 25 mM sodium phosphate buffer (pH 6.5) at 288 K. **b** Model structure of a full length subunit E of *M. jannaschii* ATP synthase. Structure of the N-terminal NMR structure $E_{1–52}$ (*red*, PDB code 2KK7, (Gayen et al. 2009)) and $E_{101–206}$ (*magenta*, PDB code 3LG8), revealing the relative positions of the two part relative to each other in the entire E subunit. The structural feature from $E_{81–100}$ (*green*) was modeled based on subunit E from *P. horikoshii* OT3 (PDB code 2DM9 (Lokanath et al. 2007)). The so far structurally unresolved segment of amino acids 53 to 100 of subunit E is highlighted as a mesh representation. The segment $E_{41–60}$, which is shown to interact with subunit H (Gayen et al. 2008), is highlighted in cyan

Acknowledgments We are grateful to the data collection facility in SPring-8 Taiwan Beamline 12B2 and SPring-8 RIKEN Beamline BL26B2. This research was supported by A*STAR BMRC (08/1/22/19/467).

References

Bernal RA, Stock D (2004) Structure 12:1789–1798
Biuković G, Rössle M, Gayen S, Mu Y, Grüber G (2007) Biochemistry 46:2070–2078
Biuković G, Gayen S, Pervushin K, Grüber G (2009) Biophys J 97:286–294
Boulin CJ, Kempf R, Koch MHJ, McLaughlin SM (1986) Nucl Instrum Methods A249:399–407
Chaban Y, Ubbink-Kok T, Keegstra W, Lolkema JS, Boekema EJ (2002) EMBO Rep 3:1–10
Collaborative Computational Project, Number 4 (1994) Acta Crystallogr D50:760–763
Coskun Ü, Grüber G, Koch MHJ, Godovac-Zimmermann J, Lemker T, Müller V (2002) J Biol Chem 277:17327–17333
Coskun Ü, Chaban YL, Lingl A, Müller V, Keegstra W, Boekema EJ, Grüber G (2004a) J Biol Chem 279:38644–38648
Coskun Ü, Radermacher M, Müller V, Ruiz T, Grüber G (2004b) J Biol Chem 279:22759–22764
Cowtan K (1994) Joint CCP4 and ESF-EACBM Newsletter on Protein Crystallography 31:34–38
DeLano WL (2002) The PyMol molecular graphics system. DeLano Scientific, Palo Alto
Emsley P, Cowtan K (2004) Acta Crystallogr D60:2126–2132
Gayen S, Grüber G (2010) FEBS Lett 584:713–718
Gayen S, Balakrishna AM, Biuković G, Yulei W, Hunke C, Grüber G (2008) FEBS J 275:1803–1812
Gayen S, Balakrishna AM, Grüber G (2009) J Bioenerg Biomembr 41:343–348
Grüber G, Marshansky V (2008) BioEssays 30:1096–1109
Grüber G, Svergun DI, Coskun Ü, Lemker T, Koch MHJ, Schägger H, Müller V (2001) Biochemistry 40:1890–1896
Grüber G, Godovac-Zimmermann J, Link TA, Coskun Ü, Rizzo VF, Betz C, Bailer S (2002) Biochem Biophys Res Commun 298:383–391
Guinier A, Fournet G (1955) Small angle Scattering of X-rays. Wiley, New York
Kish-Trier E, Wilkens S (2009) J Biol Chem 284:12031–12040
Krissinel E, Henrick K (2004) Acta Crystallogr D60:2256–2268
Kumar A, Manimekalai MSS, Balakrishna AM, Hunke C, Weigelt S, Sewald N, Grüber G (2009) Proteins 75:807–819
Laemmli UK (1970) Nature 227:680–685
Laskowski RA, MacArthur MW, Moss DS, Thornton JM (1993) J Appl Crystallogr 26:283–291
Lee LK, Stewart AG, Donohoe M, Bernal RA, Stock D (2010) Nat Struct Mol Biol 17:373–378
Lewalter K, Müller V (2006) Biochim Biophys Acta 1757:437–455
Lokanath NK, Matsuura Y, Kuroishi C, Takahashi N, Kunishima N (2007) J Mol Biol 366:933–944
Matthews BW (1968) J Mol Biol 33:491–497
McCoy AJ, Grosse-Kunstleve RW, Adams PD, Winn MD, Storoni LC, Read RJ (2007) J Appl Crystallogr 40:658–674
Müller V, Grüber G (2003) Cell Mol Life Sci 60:474–494
Murshudov GN, Vagin AA, Dodson EJ (1997) Acta Crystallogr D53:240–255
Otwinowski Z, Minor W (1997) Meth Enzymol 276:307–326
Petoukhov MV, Svergun DI (2005) Biophys J 89:1237–1250
Roessle M, Klaering R, Ristau U, Robrahn B, Jahn D, Gehrmann T, Konarev PV, Round A, Fiedler S, Hermes S, Svergun DI (2007) J Appl Crystallogr 40:190–194
Round AR, Franke D, Moritz S, Huchler R, Fritsche M, Malthan D, Klaering R, Svergun DI, Roessle M (2008) J Appl Crystallogr 41:913–917
Saff EB, Kuijlaars ABJ (1997) Math Intell 19:5–11
Schäfer I, Bailer SM, Düser MG, Börsch M, Ricardo AB, Stock D, Grüber G (2006a) J Mol Biol 358:725–740
Schäfer I, Rössle M, Biuković G, Müller V, Grüber G (2006b) J Bioenerg Biomembr 38:83–92
Svergun DI (1993) J Appl Crystallogr 26:258–267
Svergun DI (1999) Biophys J 76:2879–2886
Vonck J, Pisa KY, Morgner N, Brutschy B, Müller V (2009) J Biol Chem 284:10110–10119